Comparative classification approach in hyperion imagery

Vigneshkumar M[1], & Kiran Yarrakula[2*]

[1]PSN College of Engineering and Technology (Autonomous), Tirunelveli, India

[2]Ghani Khan Chaudhury Institute of Engineering and Technology, Malda, India

*[E-mail: kiran@gkciet.ac.in]

The traditional approaches to estimate the Iron ore involves large manpower, cost and time. Iron ore identification is necessary due to the rapid increase in construction work, industries and population. Hyperspectral Imagery analysis used to estimate the Iron ore precisely depends on the spectral signature. The spectral signature of Iron ore shows huge absorption in 865 nm due to the presence of Iron content in the sample spectra. Hyperspectral imagery contains a large number of spectral bands and involves various processing steps such as identification of the calibration bands, absolute reflectance generation, data dimensional minimization, Iron ore endmembers extraction and classification. The radiance imagery absolute reflectance bands are carried out using FLAASH atmospheric correction module. The noiseless pure pixels are obtained using data dimensionality reduction techniques as spectral data reduction and spatial data reduction. The comparative analysis is performed between sub-pixel (LSU) and per-pixel (SAM) classification. The results showed that the sub-pixel-based classification produces a better distribution of Iron ore than the per pixel-based classification.

[Keywords: FLAASH, LSU, MNF, PPI, SAM]

Introduction

Normally minerals are signified by a chemical formula that has a crystal arrangement. International Mineralogical Association (IMA) acknowledged 5070 minerals out of 5300[1]. Tamil Nadu has ample minerals such as Titanium-30 %, Molybdenum-52 %, Garnet-59 %, Dunite-69 %, Vermiculite-75 % and Lignite-81 %[2]. Iron ore identification necessity increases due to a rapid growth of population and industries. To improve the consumer and manufacturing necessities, mineral extraction is to be required. Magnetite and Hematite are very common Iron oxide (Fe_3O_4 & Fe_2O_3) minerals that are found in igneous, metamorphic, and sedimentary rocks. The prime practice of Iron ore is the invention of Iron and steel. Steel is used in cars, engines, ships, building beams, equipment, paper pins, tackles, reinforcing concrete rods, push-bikes, and additional substances[3]. In prior phases of mineral distinguishing proof depends on their physical and organic belongings. Therefore, mineral exploration is a bothersome assignment, tedious and cost-effective process. Remote sensing plays a dynamic role to recognize the minerals exactly. The process is to be carried out using hyperspectral and multi-spectral imageries. In the multispectral bands, mineral extraction is problematic due to the larger band intervals[4]. To identify the minerals properly, hyper spectral imagery has unceasing fine bands in the region of Visible, VNIR, SWIR and TR sections at short intervals. Hyper spectral imagery is used to screen vegetation mapping, mineral mapping, water quality assessment, soil moisture valuation, food quality examination etc[5]. Hyper spectral device has various space-borne sensors like Hyperion, MODIS, MERIS and IMS-1 and airborne sensors like GERIS, AVIRIS, CASI, DAIS, HYDICE, HYMAP[6]. Hyper spectral imagery requirements areas similar as calibration band separation, destriping, atmospheric alteration, data dimensionality decrease and end members identification and extraction. The spectral signature of Iron ore samples is categorized using ASD spectroradiometer. The Region from 0.4 to 1.2 μm as Visible and VNIR region of hyper spectral imagery is mainly used for abundant Iron region mapping[7]. Figure 1 demonstrates the Iron ore mineral and spectral signature curve. The major purpose of the present-day research is to compare the Iron ore mineral identification using per pixel and sub pixel classification.

Study area

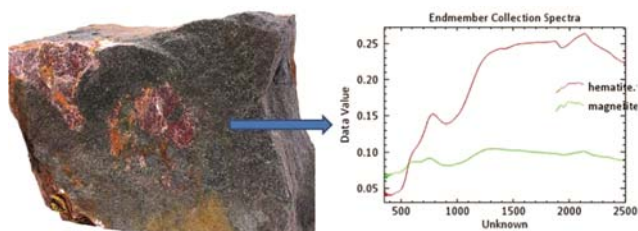The study region lies between Valapadi and Ayodhyapattanam blocks in Tamil Nadu, India. The

Fig. 1 — Iron ore mineral and its spectral sign plot

region gets abanduntIron ore such as Godumalai hills and Jarugumalai reserved forest. The study area lies in 11^0 35' 36" to 11^0 44' 59"N and 78^0 17' 21" to 78^0 22' 45" E. Figure 2 shows the topographical position of study area. Salem district has various mineral deposits such as Bauxite, Dunite, Felspar, Granite, Magnesite, Limestone, Quartz, silica, Talc, steatite, soapstone, Calcite, Chromite, Dolomite and Iron ore[3].

Data used

Hyperion

In the current research, Hyperion push broom scanner is utilized to classify the Iron ore deposit in the training area. Hyperion is a US satellite having 242 spectral bands in the range (400 nm– 2500 nm) at a 10 nm intermission and standardize in 16-bit radiometric resolution[8]. The Visible and VNIR region (400 nm – 1200 nm) of Hyperion reflectance band 1 to band 70 is used for Iron ore mapping.

ASD Spectroradiometer

Spectroradiometer is used to recognize the spectral characteristics of earth surface materials depend on their properties. In Hyperion imagery, spectroradiometer is utilized for field spectra generation, end member extraction and classification[9]. Table 1 illustrates the technical specifications of ASD Spectroradiometer.

Methodology

The significant unbiased present-day research was carried out to examine and compare various classification methods to estimate the accuracy of Iron ore deposit. Figure 3 shows the detailed methodology for identification of Iron ore minerals. In the Valapadi taluk region rock samples are collected using GPS. ASD spectroradiometer is utilized to characterize the spectral response of Iron ore. Spectroradiometer generates the spectral reflectance behavior of samples in the region of visible, VNIR (Very Near Infrared) and SWIR (Short Wave Infrared) from 400 nm – 2500 nm[10]. Hyperion imagery requires premilinary
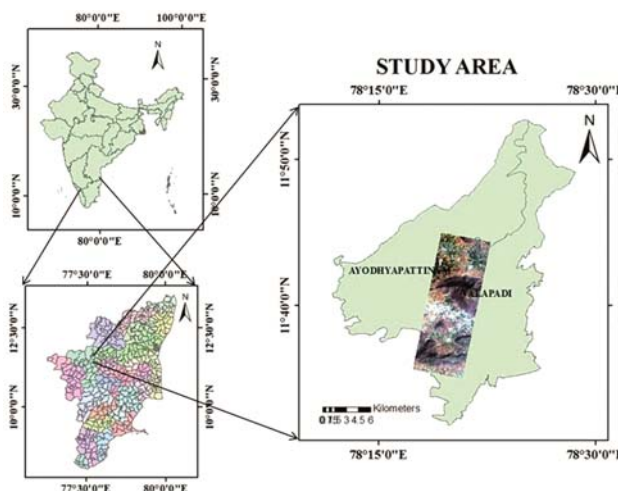

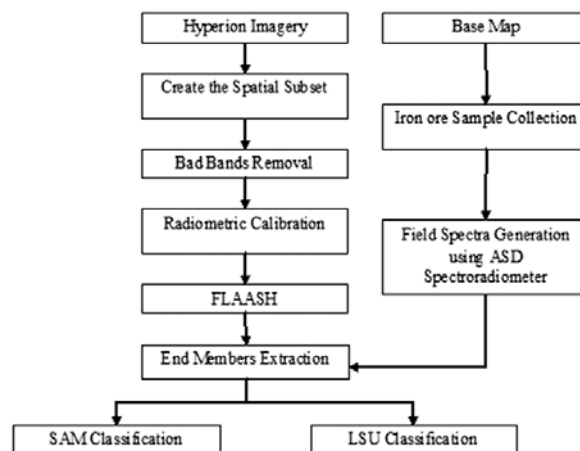Fig. 2 — Topographical position of the study area.

Fig. 3 — Methodology for the Iron ore organization using Hyperion imagery

Table 1 — Technical specifications of the ASD spectroradiometer

Variable	Technical Specifications
Spectral Range	350 nm – 2500 nm.
Sampling Interval (VNIR)	1.4 nm.
Sampling Interval (SWIR)	2 nm.
Wavelength Accuracy	0.5 nm.
Channels	2151.

processing such as identification of calibration bands, absolute reflectance generation, data dimensional minimization, Iron ore end members extraction and Iron ore abundance estimation[11].

Out of 242 bands in Hyperion imagery, 163 are in standardized level by non-illumination, and overlap regions are available in 1-7, 58-76, 225-242 bands. Hyperion data also contain noise bands by water vapor in the bands of 120-132, 165-182, 221-224[12]. The vertical columns removal are performed using

local destriping algorithm[13]. In the present study, FLAASH atmospheric module is used to generate the smooth absolute reflectance curve[14]. Data dimensonality reduction of reflectance bands are carried out using MNF and PPI. The end member signatures are identified by the high probability between the imagery spectra and field spectra. Iron ore deposit identification is performed using various classification techiniques. Finally comparitive analysis is performed between SAM and LSU classification to identify the Iron ore deposit.

Results and discussion

Iron ore spectra generation using ASD spectroradiometer

ASD spectroradiometer exemplifies the spectral signs of samples in the Visible, VNIR and SWIR regions[15]. Iron ore inorganic examples are taken in hard and dust material form for spectroradiometer examination.

ASD spectroradiometer engenders the sample spectra in wavelength region between 400 nm to 2500 nm. Due to the occurrence of iron content, sample spectra demonstrate the enormous reflectance in the region of 525 nm – 1500 nm and absorption in 865 nm. Figure 4 confirms the ASD spectroradiometer and Iron ore (Hematite) mineral spectral curve. The red line curve specifies the Hematite mineral obtainability in the samples.

Preliminary processing of Hyperion imagery identify the calibration bands in Hyperion

Hyperion imagery has a total of 242 bands, out of which 163 bands are in standardize condition, other bands are affected by noise, non-illuminated and water vapor[16]. The bands 1-7, and 225-242 are not consuming any information due to non-illuminated bands. The bands 58-76 are intersection region amid very near infrared region and shortwave infrared region. Bands 120-132, 165-182 and 221-224 are water vapor region and these bands are consuming ration of noise. Table 2 confirms the list of zero bands and bad bands in the Hyperion sensor.
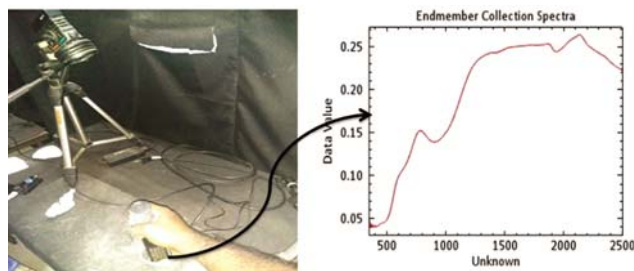

Fig. 4 — Field spectra of Hematite mineral

Destriping

In Hyperion imagery vertical column pixel standards are droplet out then it is called as striping[17]. Striping affects the quality of radiance, reflectance, data reduction methods and classification. It creates the black or white perpendicular appearances in the imagery. Vertical strips are detached using numerous approaches as filtering performances and morphological practices[18]. In the present research, VNIR section is solitary occupied for destriping process. The perpendicular strips present in the Hyperion data are detached using local destriping system and it is extremely suggested, because it adjusts barred column gray values only by locality pixel values[13].

Absolute reflectance generation

The radiometric standardization translates the radiance rate of the earth surface from the DN rate of Hyperion in the sleeve arrangement of BIL at scale factor of 0.1. The reflectance of Hyperion imageries is done using FLAASH module. By means of the complete reflectance only, it is able to recognize the Iron ore deposit consuming field spectra[19]. The absolute reflectance of Hyperion intended using FLAASH module. FLAASH is cast-off to achieve smooth absolute reflectance compared to other atmospheric modules in the region from 400 nm to 2500 nm[6]. Figure 5 demonstrates the Hyperion images and its spectral profile plot of raw image, radiance and reflectance appearances.

Data dimensionality reductions

The reflectance bands of Hyperion imagery enclose lot of noise. Noise in the reflectance bands affects the end member identification of Iron ore. MNF is carried out to identify the spectral purity information. MNF identifies the reflectance bands in the rising order depends on the noise obtainability[20]. Figure 6 (a, b) displays the noiseless and noise bands of MNF. The pixel purity index development is manipulated for each pixel in the image cube by arbitrarily

Table 2 — List of un-standardize bands in Hyperion sensor

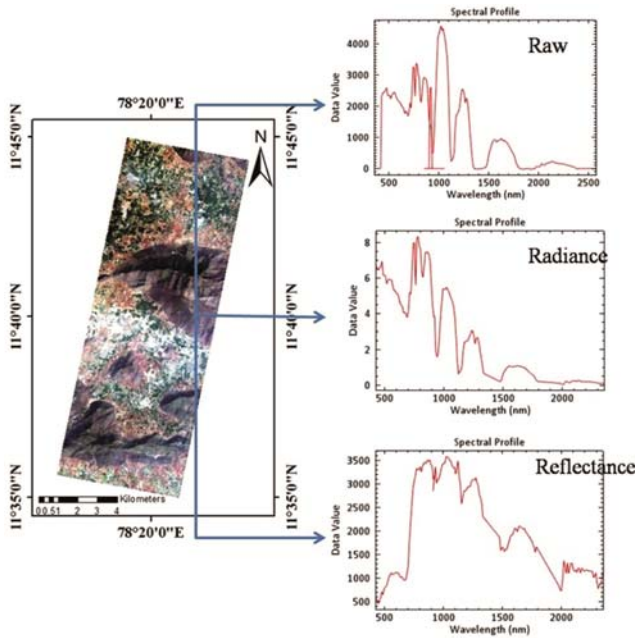| S.No	Bad bands	Reason
1	1-7	Zero bands, Non-illuminated.
2	58-76	Zero bands, Overlap region between VNIR-SWIR area.
3	121-132	Water vapor area has ration of Noise.
5	165-181	Water vapor area has ration of Noise.
6	221-224	Water vapor area has ration of Noise.
7	225-242	Zero bands, Non-illuminated.

Fig. 5 — Hyperion imagery and its spectral profile plot for raw image, radiance and reflectance
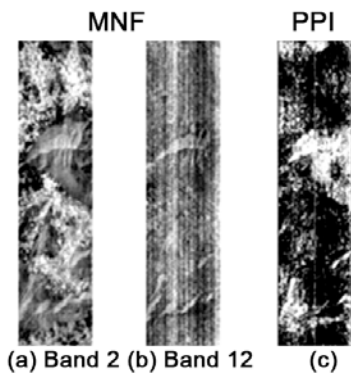

Fig. 6 — Data reduction methods of MNF and PPI

engender appearance in the N-dimensional, a distribute scheme of the MNF distorted evidence[21]. The silent bands made from MNF given as input for PPI. PPI course the MNF bands in the verge boundary of 2.5 to 10000 recurrences[11]. The black and white pixels in the PPI characterize impure and unadulterated pixels correspondingly. Figure 6c displays the spatially uncontaminated information embodied as white pixels.

End member identification

The Iron ore minerals varieties are congregated from the spectral collections of USGS, JPL and JHU. The band intermission of the collection spectra is 2.5 nm but the spectral intermission of Hyperion
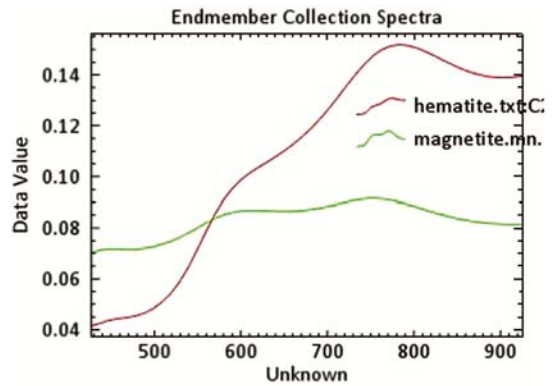

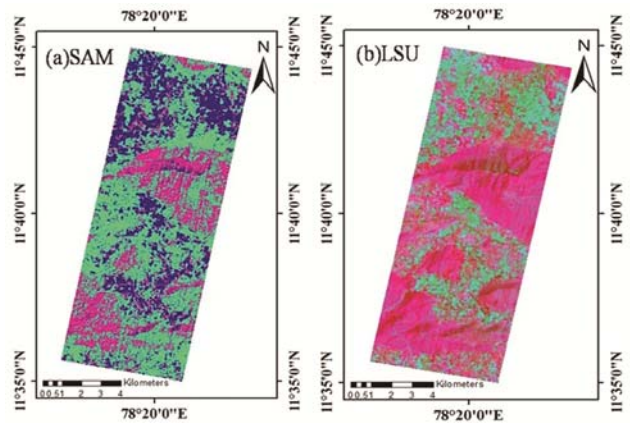Fig. 7 — Mean of end members spectral profile plot of Iron ore sample

Fig. 8 — Iron ore mapping in Hyperion using SAM and LSU classification

descriptions is 10 nm[22]. Therefore, spectral resembling approaches are implemented to amend the library spectral intermission from 2.5 nm to 10 nm intermissions. The spectral analyst associates the imagery spectra to field spectra and foodstuffs probability using the approaches such as Spectral Angle Mapper (SAM), Spectral Feature Fitting (SFF), Binary Encoding (BE). The enormous possibility scorer is taken as end member signs for classification. Figure 7 demonstrations the mean of end members spectral profile subversion for Iron ore illustration.

Spectral angle mapper (SAM)

The SAM scheme associates the image ranges and filed ranges, and it deploys the angular aloofness between the twin spectrum and the Iron ore ranges. In the Per-pixel founded organization techniques, SAM offers greater classification consequences associated to other methods. In the Hyperion imagery band assortment occupied from 400 nm to 900 nm in VNIR region every where there are 50 bands. Figure 8(a)

Table 3 — Iron ore deposit in Hyperion descriptions using SAM and LSU classification

SAM Classification			
Class	Count	Area	Percent
Hematite	55555	49.9995	48.4672
Magnetite	37615	33.8535	32.816
Uncategorized	21454	19.3086	18.7168
LSU Classification			
Hematite	66301	59.6709	57.8422
Magnetite	44527	40.0743	38.8461
Uncategorized	3796	3.4164	3.3117

shows the Iron ore mapping using SAM classification. The red pixels, green pixels and black pixels indicate the Hematite, Magnetite and other earth surface evidence, respectively.

Linear spectral unmixing (LSU)

Linear spectral unmixing is likewise done using the dual end members such as Hematite and Magnetite. Linear spectral unmixing descriptions produced for the study zone caused by giving end member orientation spectra and their profusions. LSU affords evidence about the qualified pro fusions of the end member factual considering each end member contemporary in a pixel.

Figure 8(b) demonstrates the Iron ore mapping using LSU classification. The red, green and black pixels designate the Hematite, Magnetite and other earth surface evidence respectively. The consequences of Iron ore deposit estimation in both groupings are shown in Table 3. LSU arrangement specifies the increment of Hematite, Magnetite regions from 48.47 % to 57.84 %, 32.82 % to 38.85 %, respectively. The unsystematic pixels are diminished from 18.72 % to 3.31 %.

Conclusion

In the present research, Iron ore samples such as Magnetite (Fe_3O_4) and Hematite (Fe_2O_3) spectral signatures are characterized using ASD Spectro-radiometer. The spectral curve of Iron ore shows the huge reflectance in VNIR region and absorption around 865 nm. LSU classification shows the better Iron ore deposit in the VNIR region compared to SAM. The main disadvantage in the present study is Hyperion contains low spatial resolution. The low spatial resolution affects the accuracy of Iron ore organization and their deposit approximation. In the forthcoming high spatial and spectral determination imagery such as AVIRIS proposes the sophisticated meticulousness in iron ore deposit documentation. The performance used in the present work would be an assistance to various mining, steel trades, construction, national resource management and so on.

References

1   Ramakrishnan, D., & Bharti, R, Hyperspectral remote sensing and geological applications. *Curr. Sci.*, 108(5) (2015), 879-891.

2   Vigneshkumar, M., & Yarakkula, K, Nontronite mineral identification in nilgiri hills of tamil nadu using hyperspectral remote sensing. In *IOP Conference Series: Materials Science and Engineering* (Vol. 263, No. 3, 2017, p. 032001). IOP Publishing.

3   Ganesh, B. P., Aravindan, S., Raja, S., & Thirunavukkarasu, A, Hyperspectral satellite data (Hyperion) preprocessing—a case study on banded magnetite quartzite in Godumalai Hill, Salem, Tamil Nadu, India. *Arabian J. Geosci.* 6(9) (2013), 3249-3256.

4   Magendran, T., & Sanjeevi, S., A study on the potential of satellite image-derived hyperspectral signatures to assess the grades of iron ore deposits. *J. Geol. Soci. India*, 82(3) (2013), 227-235.

5   Aravindan, S., & Ganesh, B. P., Analysis of hyperion satellite data for discrimination of banded magnetite quartzite in Godumalai Hill, Salem District, Tamil Nadu, India. *International J. Advan. Remo. Sens. GIS*, 3(1) (2014), pp-569.

6   Kumar, M. V., & Yarrakula, K., Comparison of efficient techniques of hyper-spectral image preprocessing for mineralogy and vegetation studies. *Indian J. Geo-Mar. Sci.*, 46(5) (2017), 1008-1021.

7   Dave, P. N., & Bhandari, J, Prosopis juliflora: A review. *Int. J. Chemi. Stud.*, 1(3) (2013), 181.

8   Vignesh, M., & Yarakkula, K. Identification of the Alluvial Soil Deposit Using Hyperspectral Imagery. In: *Geospatial Technol. Rural Develop.*, (2016)148-152.

9   Magendran, T., Sanjeevi, S., Bhattacharya, A. K., & Surada, S, Hyperspectral radiometry to estimate the grades of iron ores of Noamundi, India—a preliminary study. *J. Indian Soci. Remo. Sens.*, 39(4) (2011), 473-483.

10 Ballanti, L., Blesius, L., Hines, E., & Kruse, B.. Tree species classification using hyperspectral imagery: A comparison of two classifiers. *Remote Sens.*, 8(6) (2016) 445.

11 Pour, A. B., & Hashim, M. ASTER, ALI and Hyperion sensors data for lithological mapping and ore minerals exploration. *Springerplus*, 3(1) (2014) 130.

12 Vigneshkumar, M., & Kiran, Y., Spatial distribution of Prosopis juliflora using the fusion of hyperspectral and Landsat-8 OLI imagery. *Indian J. Ecol.*, 44(Special Issue 5) (2017), 548-554.

13 Pal, M. K., & Porwal, A. Destriping of Hyperion images using low-pass-filter and local-brightness-normalization. In *Geoscience and Remote Sensing Symposium (IGARSS), 2015 IEEE International* (pp. 3509-3512).

14 Minu, S., & Shetty, A. Atmospheric correction algorithms for hyperspectral imageries: A review. *Int. Res. J. Earth Sci.*, 3(5) (2015) 14-18.

15 Kumari, S. K., Debashish, C., Pulakesh, D., & Jatisankar, B. Hyperion Image Analysis for Iron Ore Mapping in Gua Iron

Ore Region, Jharkhand, India. *Int.. Res. J. Earth Sci.*, 2(9) (2014) 1-6.

16 Jung, A., Kardeván, P., & Tőkei, L. Hyperspectral technology in vegetation analysis. *Progress Agricult. Engg. Sci.*, 2(1) (2006) 95-117.

17 Xie, Y. S., Wang, J. N., & Shang, K.. An improved approach based on Moment Matching to Destriping for Hyperion data. *Procedia Environ. Sci.*, 10(2011) 319-324.

18 Tsai, F., Lin, S. Q., Rau, J. Y., Chen, L. C., & Liu, G. R. . Destriping hyperion imagery using spline interpolation. In *Proc. 26th Asian Conference on Remote Sensing* (2005, November).

19 Matthew, M. W., Adler-Golden, S. M., Berk, A., Felde, G., Anderson, G. P., Gorodetzky, D., ... & Shippert, M. . Atmospheric correction of spectral imagery: evaluation of the FLAASH algorithm with AVIRIS data. In *Applied Imagery Pattern Recognition Workshop, 2002. Proceedings. 31st* (2002, October) (pp. 157-163).

20 Pour, A. B., & Hashim, M,. Alteration mineral mapping using ETM+ and hyperion remote sensing data at Bau Gold Field, Sarawak, Malaysia. In *IOP Conference Series: Earth and Environmental Science* (Vol. 18, No. 1, (2014) p. 012149).

21 Panda, S., Banerjee, K., & Jain, M. K. Identification of Iron Ore Mines of Noamundi, Jharkhand by Using the Satellite Based Hyperspectral and Geospatial Technology. *Int. J. Sci. Res. (IJSR)*, 3(6) (2014) 149-152.

22 Lin, L., Wang, Y., Teng, J., & Wang, X. Hyperspectral analysis of soil organic matter in coal mining regions using wavelets, correlations, and partial least squares regression. *Environ. Monit. Assess.*, 188(2) (2016) 97.